Comparison between non-linear numerical models for R.C. shear walls under cyclic loading

Comparison between non-linear numerical models for R.C. shear walls under cyclic loading

Confronto tra modelli numerici non-lineari per pareti di taglio in C.A. sotto caricamento ciclico

G. Mancini[1], G. Bertagnoli[2], D. La Mazza[3], D. Gino[4]

[1,2,3,4] *Department of Buildings, Structural and Geotechnical Engineering, Politecnico di Torino, Turin, Italy*

ABSTRACT: The non-linear behaviour of concrete structures is the result of a series of phenomena, as material non-linear constitutive law and cracking process. As a consequence, in order to understand the behaviour of reinforced concrete members from elastic field to ultimate condition, is necessary to use instruments able to simulate the material damaging evolution under growing loads. Commercial non-linear finite elements codes are generally able to simulate concrete behaviour with good approximation when a progressive incremental load is applied. However, the same result could not be reached under a cyclic loading. In this work two commercial non-linear finite element codes have been considered in order to assess the skill of these codes to simulate non-linear concrete behaviour under cyclic loading. The results of six laboratory tests on shear walls have been compared with the ones obtained by means of numerical models and some conclusions on the numerical predictions are presented.

/ Il comportamento non lineare delle strutture realizzate in calcestruzzo è il risultato di una serie di fenomeni, come la non linearità della legge costitutiva del materiale ed il processo di fessurazione. Al fine di comprendere il comportamento degli elementi strutturali in calcestruzzo armato è necessario disporre di strumenti in grado di simulare il progressivo danneggiamento del materiale in presenza di carichi crescenti. In generale, i codici di calcolo presenti in commercio sono in grado di cogliere abbastanza bene il comportamento delle strutture in cemento armato soggette a carichi monotoni crescenti. Risulta invece più complesso seguire il comportamento strutturale in presenza di un carico ciclico. In questo lavoro sono stati considerati due diversi codici di calcolo non lineare agli elementi finiti al fine di verificare la loro capacità nel simulare il comportamento di pareti a taglio soggette a un carico ciclico. Sono stati considerati i risultati di sei prove di laboratorio disponibili in letteratura; tali risultati sono stati confrontati con quelli ottenuti numericamente per trarre delle conclusioni sull'affidabilità dei modelli numerici.

KEYWORDS: Reinforced concrete; non-linear; finite elements; cyclic loading; shear walls / Calcestruzzo armato; elementi finiti; non-lineare; carichi ciclici; pareti a taglio

1 INTRODUCTION

The non-linear behaviour of reinforced concrete structural members, which is expressed by the non-proportionality between actions and structural response, it is the result of a series of phenomena as non-linearity of the materials constitutive law, cracking process and second order effects into slender structures.

It is then necessary to use instruments able to follow this complex behaviour and to simulate the damaging process that occur progressively into the concrete matrix.

The Model Code 2010 allows designers to assess the structural reliability by using a safety format applicable to results coming from non-linear analysis. The structure can be considered safe if the subsequent relation is satisfied:

$$F_d \leq R_d \quad (1)$$

Where F_d = design agent action; and R_d = design strength of the structural member.

The structural response and strength can be evaluated by using GMNA (Geometrical, Material Non-linear Analysis) methods in order to take into account the real behavior under severe loading conditions.

The same analysis performed with different finite element codes can lead to discordant results, which may also show strong deviations from the experimental ones, when these are available.

Therefore, a non-linear finite element code needs to be accurately tested in order to let designers know the level of accuracy of the GMNA they will perform.

Six laboratory tests on shear walls subjected to cyclic loads up to failure are considered in this paper: Pilakoutas & Elnashai (1995) and Lefas & Kotsovos (1990).

Bertagnoli, La Mazza & Mancini (2015) presented a comparison between three commercial finite el-

ement codes named A, B and C, testing plane stress structures under monotonically increasing loads.

Software B and C demonstrated a better accuracy therefore have been chosen for the present evaluation under cyclic loads.

The shear-walls have been numerically reproduced using plane stress models, choosing the same kind of elements and the same mesh dimension in both softwares.

Commercial non-linear finite elements codes generally provide better results when used to reproduce experimental tests with monotonically increasing loads, rather than with cyclic loading.

In fact, the way the code manages cracks opening and reclosing process acquires fundamental relevance under a cyclic load configuration.

Furthermore, in reinforced concrete structures subjected to cyclic loads, becomes relevant the effect of concrete confinement provided by the member geometry and stirrups or transverse reinforcement.

Shear walls can be modelled using three-dimensional or plane stress models. Both the choices need a careful interpretation of confinement phenomena.

In particular, in plane stress models, the in-plane confinement is always managed by the f.e. code, but out-of-plane confinement effect is not taken into account automatically if the user does not introduces it artificially.

The model proposed by Eurocode 2, that will be explained in Section 3.2, has been adopted in the present paper in order to consider out-of-plane confinement contribute.

2 CASE STUDIES

2.1 *Lefas & Kotsovos walls*

The specimens realized by Lefas & Kotsovos (1990) are 650 mm wide, 1300 mm high and 65 mm thick. The walls named SW31, SW32 and SW33 have been analysed in this paper.

All specimens, tested as isolated cantilever, are monolithically connected to an upper and a lower beam, the former is used to transfer the load coming from the jack, while the latter is used to simulate a rigid foundation; in addition both elements are used to anchor vertical bars.

Figure 1 shows the nominal dimensions of the walls and the arrangement of the reinforcements. Vertical and horizontal bars with a diameter of 8 and 6.25 mm respectively have been used, furthermore the vertical edges of the walls are provided with 4 mm stirrups in order to confine the concrete.

In Tables 1-2 are summarized the main properties of the material used for each wall, where: f_{cm} is the concrete mean cylinder compressive strength, ε_{c1} is the strain at peak stress, ε_{cu1} is the ultimate strain in uniaxial loading, whereas f_y is steel yielding stress, ε_y is yielding strain, and f_u is steel failure stress and ε_u is ultimate strain.

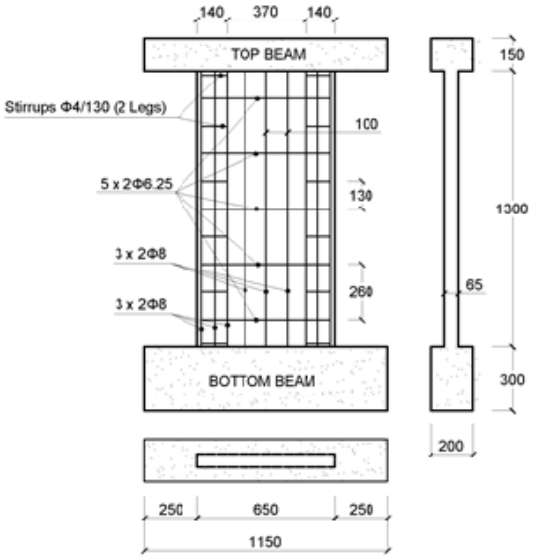

Figure 1. Geometry and reinforcement details of walls SW31, SW32 and SW33 / Geometria e dettagli delle armature per i muri SW31, SW32 e SW33.

Table 1. Concrete properties / Proprietà del calcestruzzo.

Specimen	f_{cm}	ε_{c1}	ε_{cu1}
	MPa	‰	‰
SW31	29.2	2.15	3.50
SW32	44.5	2.39	3.50
SW33	40.8	2.34	3.50

Table 2. Reinforcement properties / Proprietà delle armature.

Diameter	f_y	f_u	ε_y	ε_u
mm	MPa	MPa	%	%
Φ 4	420	490	0.21	7.50
Φ 6.25	520	610	0.26	7.50
Φ 8	470	565	0.24	7.50

Figures 2-4 show the three simplified types of horizontal cyclic loading adopted respectively for the specimens SW31, SW32 and SW33. After the cyclic phase all specimens have been incrementally loaded up to failure.

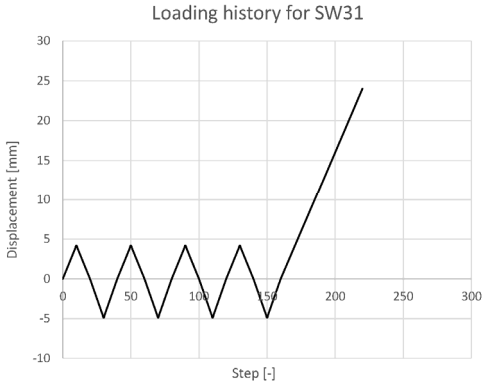

Figure 2. Loading history for wall SW31 / Storia di carico per il muro SW31.

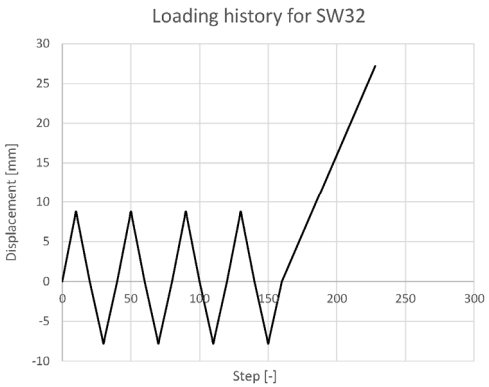

Figure 3. Loading history for wall SW32 / Storia di carico per il muro SW32.

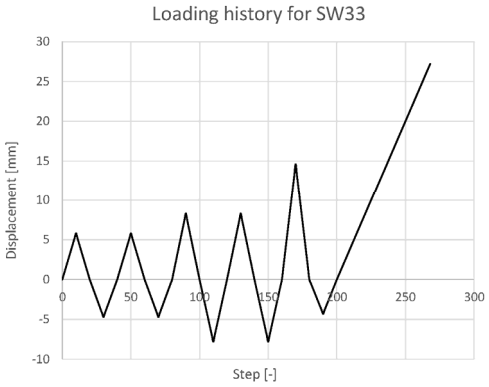

Figure 4. Loading history for wall SW33 / Storia di carico per il muro SW33.

2.2 *Pilakoutas & Elnashai walls*

The specimens realized by Pilakoutas & Elnashai (1995) are 600 mm wide, 1200 mm high and 60 mm thick; the walls named SW4, SW6 and SW8 have been analysed in the present work.

The horizontal force coming from the jack has been applied to a top beam designed to diffuse it uniformly into the wall.

The load scheme presented in Pilakoutas paper shows also the presence of two rollers placed at the sides of the upper beam and connected to a vertical steel frame in order to control the horizontal movement of the top beam.

Detailed information about these devices are not given in the paper, therefore the authors performed several simulations with different constraint conditions at the top of the walls.

The best fitting with experimental results has been obtained with nil vertical constraints applied to the top beam.

The walls are fully restrained and anchored to a lower beam used to simulate a rigid foundation; the upper and lower beams are also used to anchor the vertical reinforcement bars.

Figures 5-7 show the nominal dimensions of the walls and the arrangement of the reinforcements. Vertical and horizontal bars with a diameter between 4 and 12 mm have been used; two "pillars" at the sides of the walls are provided with stirrups with a diameter of 4 and 6 mm, each walls has a different disposition of the stirrups.

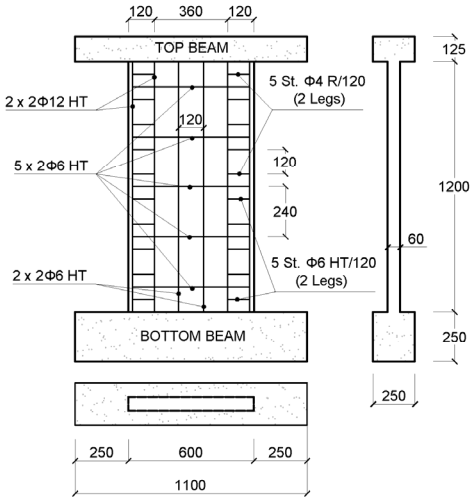

Figure 5. Geometry and reinforcement details of wall SW4 / Geometria e dettagli delle armature per il muro SW4.

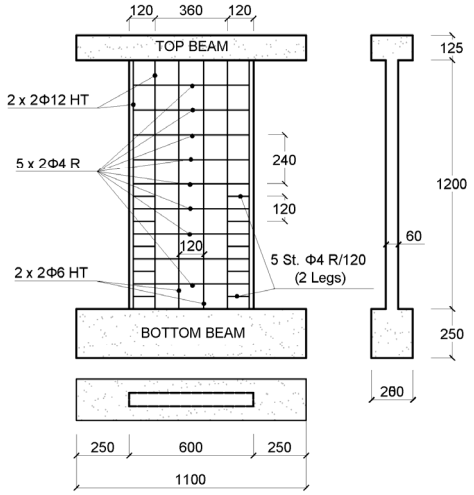

Figure 6. Geometry and reinforcement details of wall SW6 / Geometria e dettagli delle armature per il muro SW6.

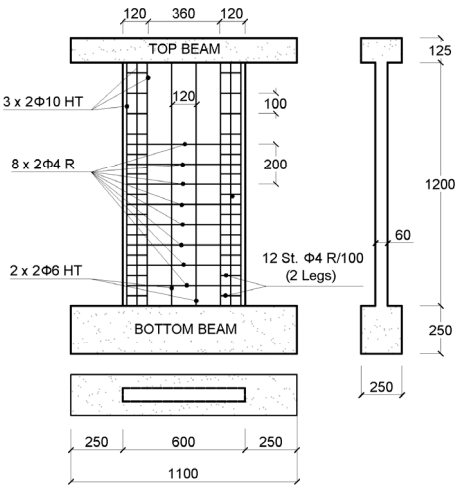

Figure 7. Geometry and reinforcement details of wall SW8 / Geometria e dettagli delle armature per il muro SW8.

In Table 3-4 are summarized the main properties of the material used for each wall. The meaning of

the symbols has been already described in the previous paragraph.

Table 3. Concrete properties / Proprietà del calcestruzzo.

Specimen	f_{cm}	ε_{c1}	ε_{cu1}
	MPa	‰	‰
SW4	36.9	2.28	3.50
SW6	38.6	2.30	3.50
SW8	45.8	2.41	3.50

Table 4. Reinforcement properties / Proprietà delle armature.

Diameter	f_y	f_u	ε_y	ε_u
mm	MPa	MPa	%	%
Φ 4	400	460	0.20	6.00
Φ 6	545	590	0.27	2.00
Φ 10	530	660	0.27	4.20
Φ 12	500	660	0.25	8.50

Figure 8 shows the loading history adopted for SW4, SW6 and SW8. A single load level is composed by two full cycles with the same maximum top displacement. When one load level is completed the top displacement has been incremented of 2 mm in both directions.All specimens have been tested up to failure.

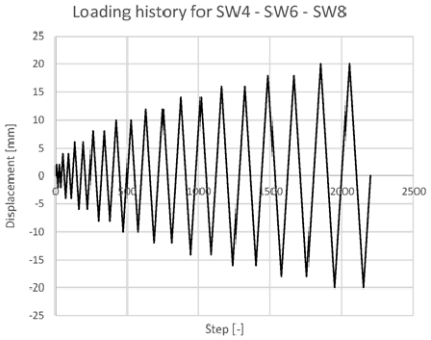

Figure 8. Geometry and reinforcement details of wall SW4 / Geometria e dettagli delle armature per il muro SW4.

3 FINITE ELEMENTS MODELS

3.1 *Mesh and material models*

Numerical models of the shear walls have been realized using four-node quadrilateral isoparametric plane stress finite elements, based on linear polynomial interpolation and 2x2 Gauss point's integration scheme. The dimension of each element is about of 0.05 x 0.05 m, this size has been chosen after a calibration procedure.

The main mechanical characteristics of the material models used in the codes are the same defined in Bertagnoli, La Mazza & Mancini (2015), the only differences are:

- In Software C, the constitutive law adopted for concrete follows EN1992-1-1 instead of the Thorenfeld law;
- In Software B and C, the shear stiffness reduction after cracking has been considered by means of a shear retention factor $\beta = 0.15$.
- In Software B and C, the concrete tensile behaviour has been modelled with a linear tension softening law only. The latter presents the ultimate strain of softening branch as $10 \cdot \varepsilon_l$. Where ε_l is the strain corresponding to the peak concrete tensile strength.

3.2 *Out-of-plane confinement*

The out-of-plane confinement action given by the closed stirrups located along the external chords of the shear walls, can provide an important stiffening contribute, particularly in presence of cyclic loading.

In the present work has been adopted the model proposed by Eurocode 2 in order to consider this favourable effect as already proposed by the authors (Bertagnoli, Mancini, Recupero & Spinella (2011)).
Out-of-plane confinement has been taken into account by increasing the peak strength, the corresponding strain and the ultimate compression strain in the constitutive law for concrete in compression. The increase in strength and both in ultimate and peak strains of concrete depends on the effective transverse compressive stress that has been estimated as a function of the amount of the out-of-plane reinforcement ρ_z and its deformation level ε_z .
Out-of-plane reinforcement can be evaluated as the shear link leg area A_{st} smeared on the confined chords width cs ($\rho_z = A_{st}/cs$).

The stress $\sigma_{s,z}$ in the transverse reinforcement can be evaluated by an approximated approach using an elastic-plastic law:

$$\sigma_{s,z} = \begin{cases} E_s \cdot \varepsilon_z & if \quad \varepsilon_z < \varepsilon_{s,y} \\ f_y & if \quad \varepsilon_z \geq \varepsilon_{s,y} \end{cases} \tag{2}$$

Where ε_z = out-of-plane strain from plane stress theory. Thus, the confining stress σ_z in concrete has been calculated as follows:

$$\sigma_z = -\rho_z \cdot \sigma_{s,z} \tag{3}$$

The effect of confining stresses is a strength enhancement:

$$f_{cm,c} = f_{cm}\left(1 + 5\sigma_z / f_{cm}\right) \quad if \quad \sigma_z < 0.05 f_{cm} \tag{4}$$

$$f_{cm,c} = f_{cm}\left(1.125 + 2.5\sigma_z / f_{cm}\right) \; if \; \sigma_z > 0.05 f_{cm} \quad (5)$$

Where $f_{cm,c}$ = average cylindrical strength of confined concrete; f_{cm} = average cylindrical strength from a uniaxial test.

The strain at peak strength $\varepsilon_{c0,c}$ and the ultimate strain $\varepsilon_{cu,c}$ in the confined state are related to the respective unconfined values as follows:

$$\varepsilon_{c0,c} = \varepsilon_{c0}\left(f_{cm,c} / f_{cm}\right)^2 \quad (6)$$

$$\varepsilon_{cu,c} = \varepsilon_{cu} + 0.2\sigma_z / f_{cm} \quad (7)$$

4 RESULTS DISCUSSION

The results obtained respectively with software B, software C and the experimental ones are shown side by side in Figures 9-26 in order to allow an easy interpretation.

All numerical models have been loaded applying an imposed horizontal displacement to the top beam and the comparison between experimental and numerical results is done in terms of horizontal force corresponding to the imposed displacement (jack force).

The results of walls SW31, SW32, SW33 turn out to be more accurate and faithful to experimental ones than walls SW4, SW8, SW10.

The main difference between the two families of walls is the loading processes as described in section 2.

4.1 *Software B results*

- SW4: the model is able to reproduce adequately the experimental behaviour only up to an imposed displacement of the top beam of ±14 mm (maximum displacement applied during the experimental test = ±20 mm). For higher displacements software C is not able to provide reliable results.
  However, especially for high displacement levels, the numerical prediction of the applied force differs from the experimental one only of ±5%.
- SW6: the model is able to reproduce adequately the experimental behaviour only up to an imposed displacement of the top beam of ±14 mm (maximum displacement applied during the test = ±20 mm). The applied load is overestimated of about 20% for higher imposed displacements.
- SW8: the model is able to reproduce adequately the experimental behaviour only up to an imposed displacement of the top beam of ±10 mm (maximum displacement applied during the test = ±20 mm). the load is overestimated again of about +25%. The model is stiffer in the initial stages but becomes too deformable for higher displacements.
- SW31: the model is able to reproduce adequately the experimental behaviour for the whole test. As regards the cyclic stage, during the loading phases it can be noted a good correspondence with the actual values, while in the unloading phases the response of the software B can be considered elastic. Nevertheless an underestimation of the ultimate load of about 20% has to be declared.
- SW32: the model is able to reproduce adequately the experimental behaviour for the whole test. In last stage up to the failure, software B is able to reproduce the actual behaviour, but also in this test there is an underestimation of the ultimate load of about 10%;
- SW33: Similar considerations to the previous case can also be done for this wall. It can be noticed a small underestimation of the experimental load of about 10% during the cycles, whereas in the final loading up to failure there is an underestimation of the ultimate load of about 15%. The global behaviour is although well reproduced.

4.2 *Software C results*

- SW4: the numerical model is able to reproduce adequately the experimental behaviour only up to an imposed displacement of the top beam of ±16 mm (maximum displacement applied during the experimental test = ±20 mm). For higher displacements software C is not able to provide reliable results.
  The amplitude of the cycles, as well as the slope of the loading and unloading curves, are approximated in a satisfactory way. However, especially for high displacements, the corresponding loads are greater than the experimental ones (deviation between +5% and +20%). The numerical model seems to be stiffer than the experimental one especially in the first part of the analysis.
- SW6: as for wall SW4, the numerical model is able to reproduce adequately the experimental behaviour only up to an imposed displacement of the top beam of ±16 mm (maximum displacement applied during the test = ±20 mm). For higher displacements with software C it can be noted the presence of high shear deformation localized at the base which is not in accordance with the experimental results.
- SW8: the numerical model is able to reproduce adequately the experimental behaviour only up to an imposed displacement of the top beam of ±12 mm (maximum displacement applied during the test = ±20 mm). A progressive softening can be noted for higher imposed displacements, resulting in flattening of loading and unloading cycles; this phenomenon is not in accordance with the experimental behaviour.

The prediction of the applied horizontal force is correct up to ±12 mm of displacement, whereas the numerical model becomes too deformable for higher imposed displacements.

– SW31: the numerical model is able to reproduce adequately the experimental behaviour in the whole test. A good correspondence with the experimental values of force and displacement can be observed in the cyclic stage in the loading curves, while some disagreement between numerical and experimental can be seen in the unloading curves as the response of the software C can be considered elastic during unloading. In the last part of the test, software C is able to reproduce the experimental behaviour in a satisfactory way up to failure, however it underestimates the ultimate load of about 20%.

– SW32: the numerical model is able to reproduce adequately the experimental behaviour in the whole test. In the cyclic stage, the model response is very good both during the loading phases and the unloading ones, unlike SW31. Finally, in last stage up to the failure, software C is able to reproduce the actual behaviour, also in this test there is an underestimation of the ultimate load, but the difference is less than 10%.

– SW33: the same considerations seen in the previous case can be drawn also for this wall. The amplitude of the cycles, as well as the slope of the loading and unloading curves, are approximated in a satisfactory way for the whole duration of test. Again, a small underestimation (about 10%) of the ultimate load can be noted. During the last loading curve up to the failure, software C is able to reproduce the actual behaviour up to 20mm of imposed displacement, whereas the experimental test reached 25mm. A slight underestimation of the ultimate load (10%) is found again.

Software B and Software C show a substantial equivalence in the simulation of the structural behaviour.

A relevant parameter to evaluate performance of the numerical analyses seems to be the ratio between the top horizontal displacement and the height of the wall, which can be called “shear deformation”.

In fact, it represents the global average level of angular distortion γ that occur into the wall during the test.

Solutions proposed by Software B and C are satisfactory until the parameter γ reaches a value around $8 \cdot 10^{-3}$, which, being all the walls height almost equal, corresponds to a top horizontal displacement of about 10 mm.

Such value of γ implies a principal deformation ε_2 magnitude which is close to the deformation at failure of concrete ($\approx 3.5 \cdot 10^{-3}$).

When γ level of angular distortion is passed, both software are unable to reproduce accurately the actual structural behaviour.

For high displacement levels, the phenomena connected to confinement effect due to both reinforcements and two-dimensional behaviour become relevant and material non-linearities are particularly uncertain.

A second parameter which plays an important role in governing the numerical results is the shear retention factor β.

The factor β is the ratio between the shear modulus G in cracked and uncracked state. High values of β ($0.2<\beta<0.5$) imply big hysteresis cycles, whereas low values ($\beta<0.15$) give rise to “slimmer” curves and low levels of dissipated energy. Parameter β can be variable according to the strain level, but it has been kept constant in this work in order to compare software B and C results more accurately.

5 CONCLUSIONS

The present work has analysed the uncertainties of the outcome of different non-linear analysis of reinforced concrete shear walls subjected to horizontal cyclic loading. Two different finite element software have been used to simulate the behaviour of two distinct triplets of walls.

Quite good accuracy and small scattering of the results have been achieved for cycles having a shear deformation up to $8 \cdot 10^{-3}$, whereas for higher loading levels it has been found a loss of accuracy of the results. Shear retention factor deeply governs the amount of dissipated energy controlling the hysteretic behaviour.

Further development of the research will consider the influence of more FE model parameters on the prediction of the structural response.

Nel presente lavoro sono state analizzate le incertezze che derivano dai risultati di un’analisi non lineare agli elementi finiti su pareti di taglio soggette a carichi ciclici. A tal fine, sono stati considerati due noti software di calcolo per simulare la risposta strutturale di due diverse triplette di pareti.

Una buona accuratezza nei risultati è stata riscontrata fino a cicli con livelli di distorsione a taglio di $8 \cdot 10^{-3}$, mentre per livelli di spostamento superiori è stata riscontrata una perdita di accuratezza nella soluzione. La rigidezza a taglio in campo fessurato si è dimostrata essere un parametro fondamentale nella corretta interpretazione del comportamento isteretico delle strutture.

Ulteriori sviluppi di tale ricerca vorranno considerare l’influenza di più parametri sulla predizione della reale risposta strutturale tramite l’analisi non lineare FEM.

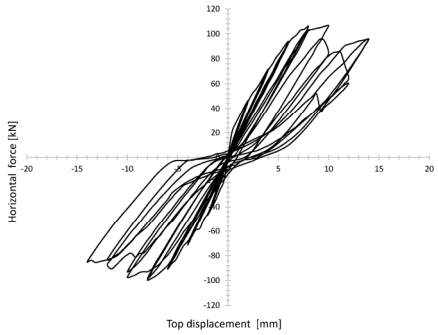

Figure 9. Software B: force Vs displacement SW4 / Software B: forza vs spostamento SW4.

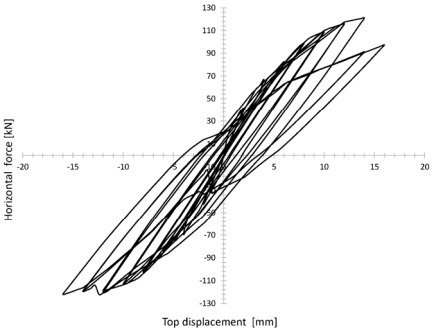

Figure 10. Software C: force vs displacement SW4 / Software C: forza vs spostamento SW4.

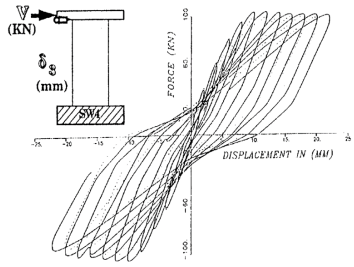

Figure 11. Experimental: force vs displacement SW4 / Sperimentale: forza vs spostamento SW4.

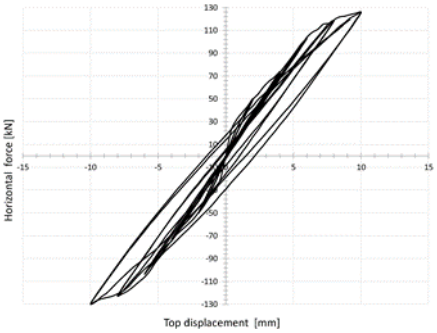

Figure 12. Software B: force vs displacement SW6 / Software B: forza vs spostamento SW6.

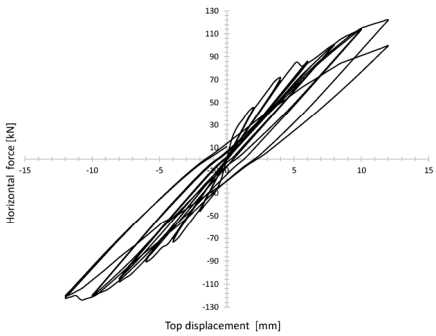

Figure 13. Software C: force vs displacement SW6 / Software C: forza vs spostamento SW6.

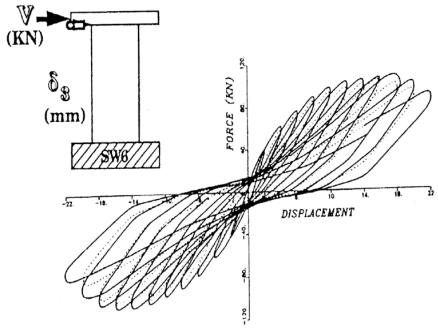

Figure 14. Experimental: force vs displacement SW6 / Sperimentale: forza vs spostamento SW6.

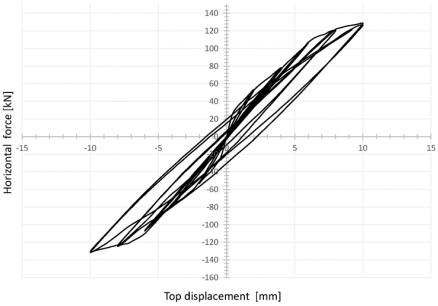

Figure 15. Software B: force vs displacement SW8 / Software B: forza vs spostamento SW8.

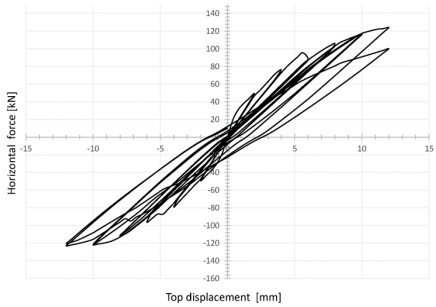

Figure 16. Software C: force vs displacement SW8 / Software C: forza vs spostamento SW8.

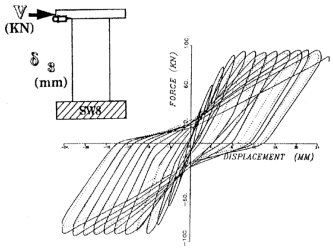

Figure 17. Experimental: force vs displacement SW8 / Sperimentale: forza vs spostamento SW8.

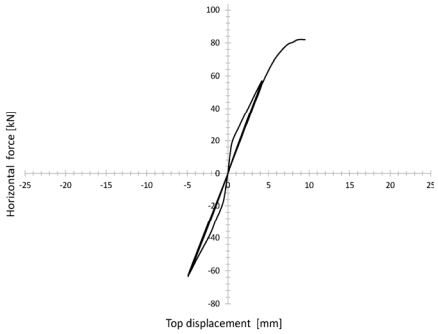

Figure 18. Software B: force vs displacement SW31 / Software B: forza vs spostamento SW31.

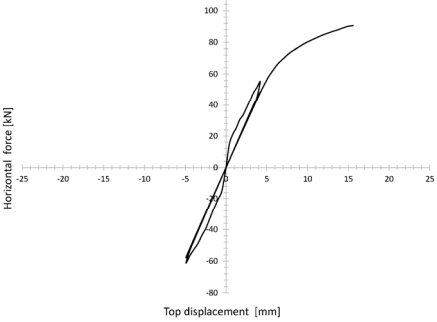

Figure 19. Software C: force vs displacement SW31 / Software C: forza vs spostamento SW31.

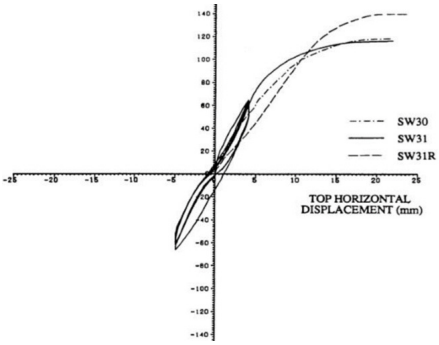

Figure 20. Experimental: force vs displacement SW31 / Sperimentale: forza vs spostamento SW31.

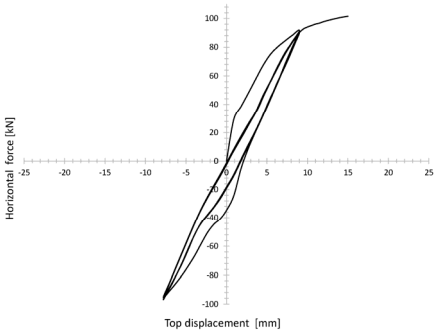

Figure 21. Software B: force vs displacement SW32 / Software B: forza vs spostamento SW32.

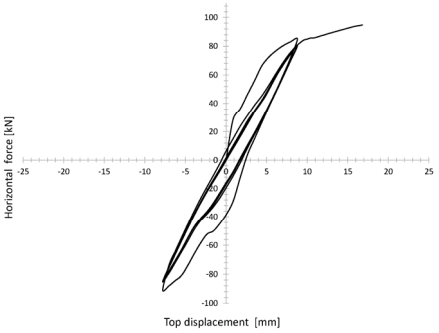

Figure 22. Software C: force vs displacement SW32 / Software C: forza vs spostamento SW32.

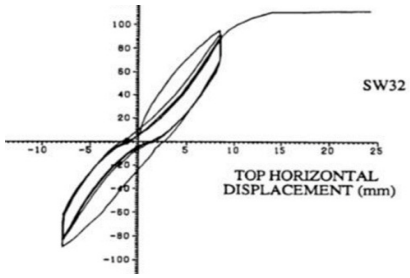

Figure 23. Experimental: force vs displacement SW32 / Sperimentale: forza vs spostamento SW32.

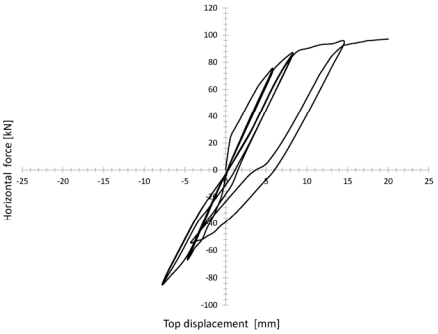

Figure 24. Software B: force vs displacement SW33 / Software B: forza vs spostamento SW33.

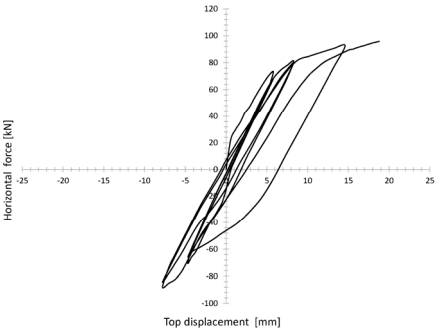

Figure 25. Software C: force vs displacement SW33 / Software C: forza vs spostamento SW33.

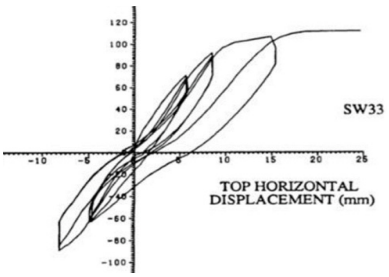

Figure 26. Experimental: force vs displacement SW33 / Sperimentale: forza vs spostamento SW33.

.

6 REFERENCES

Pilakoutas, K. & Elnashai, A. 1995. Ciclyc behaviour of reinforced concrete cantilever walls, part I: experimental results. *ACI structural journal, technical paper, Title No. 92-S25, 271-281.*

Lefas, I.D. & Kotsovos, M.D. 1990. Strength and deformations characteristics of reinforced concrete walls under load reversals. *ACI structural journal, technical paper, Title No. 87-S74, 716-726.*

Bertagnoli, G. La Mazza, D. & Mancini, G. 2015. Effect of concrete tensile strenght in non linear analyses of 2D structures - a comparison between three commercial finite element softwares.

Bertagnoli, G. Mancini, G. Recupero, A. & Spinella, N. 2011. Rotating compression fields for reinforced concrete beams under prevalent shear actions. *Structural concrete 12 (2011), No. 3, 178-186..*

Kupfer, H.B & Gerstle, H.K. 1973. Behavior of Concrete under Biaxial Stresses. *Journal Engineering Mechanics Division, Vol. 99, No. 4.*

CEB-FIP Model Code 1990, First Draft. *Committee Euro-International du Beton, Bulletin d'information No. 195, 196.*

Eurocode 2, EN 1992-1-1 2004. Design of Concrete Structures *– Part.1: General rules and rules for buildings*.